DESIGN AND OPTIMIZATION OF A SYNERGISTIC NANOPARTICLE DELIVERY SYSTEM COMBINING CHEMODYNAMIC THERAPY AND PHOTOTHERMAL THERAPY

Weiwei CHENG[1.2.3*]

In response to the endogenous H_2O_2 deficiency in the tumor microenvironment and limited efficacy of single-mode therapy, a nanomedicine delivery system combining chemodynamic therapy and photothermal therapy is designed. The in vitro test results showed that the system had significant photothermal performance. Under 800nm laser irradiation, the 0.5mg/mL supramolecular nanovalve solution heated up to 36℃ within 5 minutes, with a photothermal conversion efficiency of 32.4%, and maintained stable photothermal response after 3 cycles. Cell toxicity tests showed that the system could effectively inhibit tumor cell viability and exhibit concentration and time-dependent effects. After incubation at a concentration of 64μg/mL for 48 hours, the cell viability of the intact supramolecular nanovalve decreased to 10.2%, significantly lower than that of the control group lacking ascorbyl palmitate or photosensitizer, indicating its synergistic therapeutic effect. This study significantly inhibits tumor growth, provides innovative methods for addressing tumor drug resistance and recurrence, and opens up new avenues for improving the precision and effectiveness of tumor treatment.

Keywords: nanomedicine; chemodynamic therapy; photothermal therapy; delivery system

1. Background

Cancer treatment has long faced challenges such as insufficient specificity of traditional therapies, high systemic toxicity, and susceptibility to drug resistance. Nanoparticle Drug Delivery Systems (NDDS) modify nanocarriers to have targeting properties, accurately delivering drugs to diseased cells and reducing damage to normal tissues [1]. Chemodynamic Therapy (CDT) relies on endogenous H_2O_2 without external energy and has strong selectivity [2]. However, the H_2O_2 content in solid tumors is often lower than the threshold required for the reaction,

[1] Medical School, Xi'an Peihua University, Xi'an, 710125, China
[2] Youth Innovation Team of Shaanxi Universities, Brain Injury and Repair Research Team, Xi'an Peihua University, Xi'an, 710125, China
[3] * Key Laboratory of Shaanxi Universities, Brain Injury and Drug Prevention Research Laboratory, Xi'an Peihua University, Xi'an, 710125, China, corresponding author, e-mail: cww1232025@126.com

and the upregulation of antioxidant networks such as glutathione rapidly clears free radicals, significantly weakening the sustained efficacy of CDT [3]. Photothermal Therapy (PTT) uses photothermal agents excited by Near-Infrared (NIR) to generate high temperatures locally for tumor ablation, which has the advantages of temporal and spatial controllability and rapid killing [4].

Many researchers have solved key issues in medical drugs and diagnosis and treatment through different NDDS strategies. For example, Q. Li et al. overcame the shortcomings of poor water solubility and low stability of active ingredients in traditional Chinese medicine using self-assembly methods and mechanisms of natural small molecule compounds such as terpenes, flavonoids, alkaloids, and their application in NDDS. The results showed that this method had bioavailability and therapeutic efficacy [5]. M. Shen et al. proposed a dual-mode diagnostic and therapeutic integrated probe with hydrogen peroxide response for the diagnosis and treatment of atherosclerosis, and relied on NDDS to release drugs in the plaque microenvironment. The results showed that this method had good therapeutic effect [6]. D. Birla et al. optimized key parameters such as system particle size, zeta potential, and encapsulation efficiency using the quality-based design method to achieve the industrial development of NDDS. The results showed that the nano formulation of this method had good quality stability and therapeutic efficacy [7]. R. Mirza et al. aimed at the rapid elimination rate of cefepime and poor patient compliance, and prepared cefepime nano transfer by rotary evaporation ultrasound method. The parameters were optimized based on Box Behnken model, loaded into chitosan gel, and a transdermal drug delivery system was developed. The results showed that the system had sustained release characteristics, high skin permeability, and good biocompatibility [8]. C. Yan et al. constructed a Targeting Group for Neurodegeneration (TGN) modified red blood cell membrane coated polylactic acid hydroxyacetic acid nanoparticle to overcome the blood-brain barrier drug delivery challenge in Alzheimer's disease, and promoted synaptic plasticity in hippocampal neurons. The results showed that it could increase the recognition index from 0.275 to 0.414 [9].

In recent years, the combination of CDT and PTT has received attention, and some researchers have used NDDS to achieve precise treatment. Among them, J. Wu et al. designed a platinum cobalt @ manganese dioxide nano antibacterial platform containing PTT and CDT functions to overcome bacterial resistance. The platform utilized its photothermal effect to disrupt bacterial membrane permeability, catalyze hydroxyl radicals to kill bacteria, and alleviate the hypoxic environment in the infected area. The experiment confirmed that this method had excellent antibacterial performance and good biocompatibility [10]. X.X. Wu et al. developed a precise and controllable NDDS by constructing a gold nanoparticle co-delivery system loaded with paclitaxel through a dynamic covalent self-assembly strategy of thiol-disulfide bond exchange reaction. The experiment confirmed that

it had significant chemotherapy photothermal synergistic anti-tumor effects [11]. G. Qian et al. prepared a composite bone scaffold using selective laser sintering technology to eliminate microbial biofilms. The acidic biofilm microenvironment was used to trigger the decomposition of ZnS, releasing H2S gas to destroy the biofilm structure. The synergistic photothermal effect of MXene was used to achieve gas/photothermal combined therapy. The experiment showed that the E. coli clearance rate of the scaffold reached 90.4% [12]. G. Ma et al. developed an efficient nanoplatform for tumor therapy applications by constructing a polydopamine coated manganese sulfide nanocluster. Based on its pH responsiveness, H2S gas was released to inhibit mitochondrial respiration, synergizing Mn2+ induced iron death and dopamine photothermal effects. The results showed that this method enhanced imaging and photothermal efficacy [13]. Z. Zhang et al. aimed at developing multi-modal synergistic anti-tumor therapy, combined PTT with heat shock protein inhibitor, and used rare earth doped optical fiber to break through the tissue penetration depth limit and directly reach the tumor focus. The photothermal response hydrogel was utilized to control the released inhibitor to reduce tumor heat resistance. The results confirmed that this method could completely eliminate tumors [14].

In summary, the existing NDDS has good performance. Considering the current insufficient H_2O_2 supply, single spectrum of reactive oxygen species, and poor targeted enrichment efficiency, it is difficult to fully unleash the synergistic potential of CDT and PTT. Therefore, a novel NDDS is designed. To ensure the specific implementation of this design, a Supramolecular Nanovalves (SN) based on Mesoporous Silica Nanoparticles (MSNPs) as carriers is constructed, namely MSNPs-SN. The research aims to improve the efficacy of tumor treatment and provide a more effective biotechnology for tumor treatment.

2. Research design

2.1. Construction of NDDS and design of nanocarriers

Relying solely on a single method of H_2O_2 supplementation is insufficient. In order to improve the therapeutic effect of CDT, the NDDS designed in this study aims to integrate CDT and PTT functions, requiring core functional modules such as targeted delivery module, self supplied H_2O_2 module, CDT module, PTT module, etc. Based on these functional designs, a specific type of MSNPs SN was developed, which consisted of MSNPs, $Fe(C_5H_5)_2$, Ascorbyl Palmitate (AP), Infrared 825 (IR825), and β-Hyaluronic Acid Cyclodextrin (β-HACD). The reaction route of MSNPs-SN material synthesis is shown in Fig. 1.

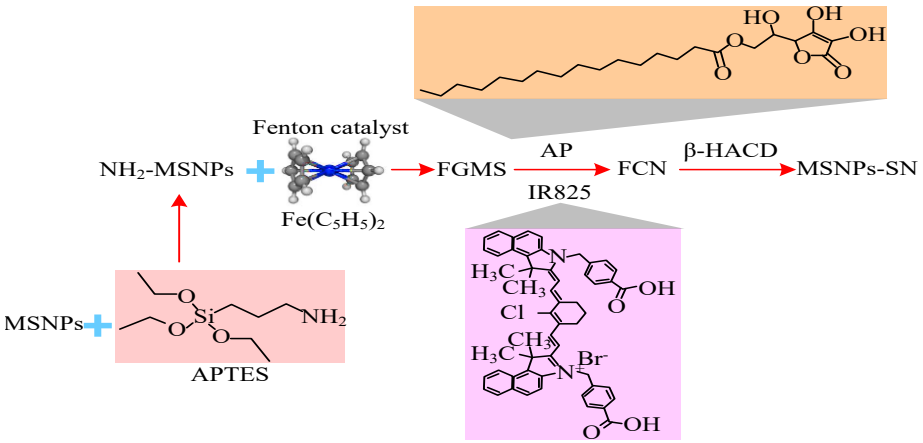

Fig. 1. Reaction routes for the synthesis of MSNPs SN materials

In Fig. 1, MSNPs undergo amination under the action of 3-Aminopropyltriethoxysilane (APTES). To construct the CDT functional core of the system, $Fe(C_5H_5)_2$ was grafted onto MSNPs through coupling reaction to obtain Ferrocene grafted mesoporous silica (FGMS). Under adsorption, AP and IR825 are loaded into the porous environment of FGMS to obtain FGMS Composite Nanomaterials (FCN). The host guest interaction between Carbon Dots (CDs) and Fe(C5H5)2 results in the MSNPs-SN by covering β-HACD on the surface of FCN. After administering medication to experimental mice, the nanoparticles exert their effects within tumor cells. AP oxidizes to produce H_2O_2, which is then converted into Reactive Oxygen Species (ROS) such as ·OH through the Fenton reaction [15]. The schematic diagram of the synergistic therapeutic chemobiological mechanism and multimodal anti-tumor mechanism of NDDS is shown in Fig. 2.

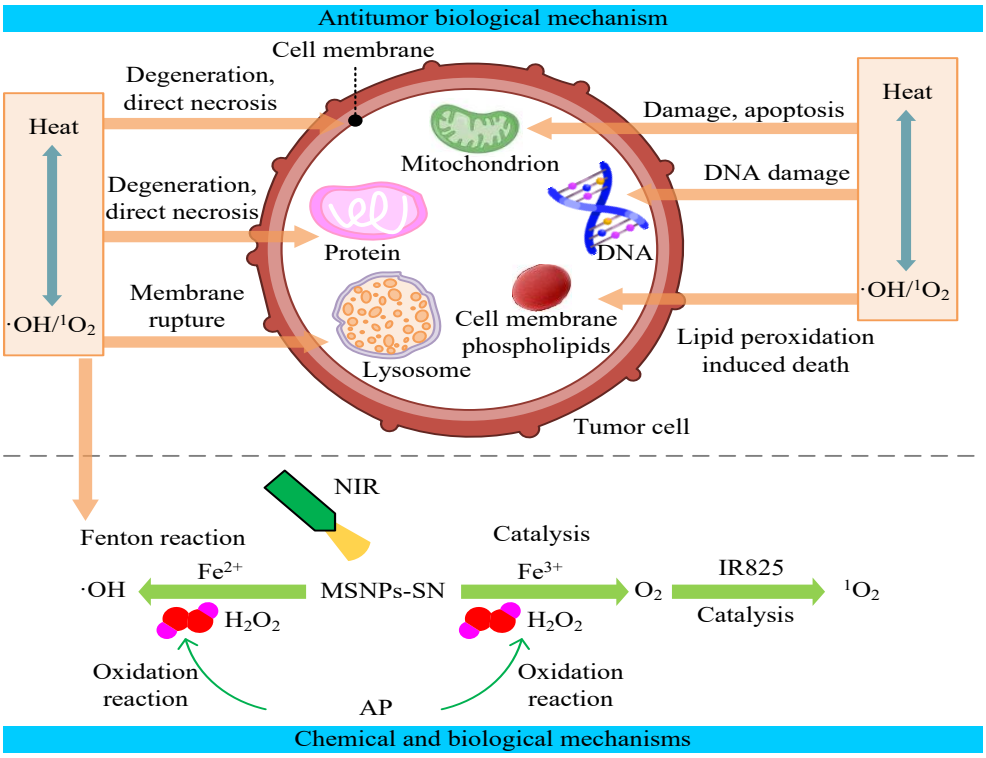

Fig. 2. Schematic diagram of NDDS synergistic therapy mechanism

In terms of the chemical biology mechanism in Fig. 2, after the NDDS system enters the tumor microenvironment, the internally loaded AP and IR825 react under specific stimuli, causing changes in the system state and inducing therapeutic effects. AP participates in the reaction cycle during two oxidation processes. Fe^{2+} utilizes H_2O_2 to generate ·OH through Fenton reaction, promoting the oxidative damage process related to treatment [16]. Fe^{3+} uses H_2O_2 for catalytic reaction to generate O_2. IR825 generates $^1O_2$ through catalysis with the participation of O_2. $^1O_2$ is an reactive oxygen species that can exert therapeutic effects such as killing diseased cells. The laser source emits laser, causing MSNPs-SN to produce photothermal effect. Photothermal can directly ablate lesions and also assist in enhancing chemical reaction efficiency, achieving synergistic treatment. In the anti-tumor mechanism, Heat can cause protein denaturation and damage to the cell membrane of tumor cells, inducing rapid and direct necrosis. Meanwhile, high fever can also damage lysosomal membranes, causing their contents to leak into the cytoplasm and accelerating cell death. The generated ·OH and $^1O_2$ cause extensive oxidative damage to key cellular components, such as ·OH attacking mitochondrial membranes, leading to membrane potential collapse, releasing cytochrome C, and triggering cell apoptosis. Heat can also directly damage the function of

mitochondria. Nanoparticles are often ingested by cells through endocytosis and enter lysosomes. The photothermal effect can cause the rupture of lysosomal membranes, releasing acidic hydrolytic enzymes into the cytoplasm, leading to cell autolysis. High levels of ROS can penetrate the nucleus, causing DeoxyriboNucleic Acid (DNA) strand breakage and damage, leading to cell apoptosis. Fe^{2+} in the system generates ·OH through the Fenton reaction, which can trigger lipid peroxidation on the cell membrane, leading to ferroptosis and achieving multi-mode, synergistic lethal strikes on tumor cells.

2.2. Preparation process of nanocarriers

MSNPs were synthesized using a sol-gel method using CTAB as the template and TEOS as the silica source, followed by removal of the template. The obtained MSNPs were then functionalized with amino groups using APTES to form NH2-MSNPs. Ferrocene was grafted onto NH2-MSNPs via condensation reaction to obtain FGMS. AP and IR825 are co-loaded into the pores of FGMS through adsorption in ethanol, thereby forming an FCN composite. Finally, FCN was coated with β-HCAD through the host-guest interaction between cyclodextrin and ferrocene to form targeted MSNPs-SN.

2.3. Performance testing methods

2.3.1. H_2O_2 generation ability test

The study selects a real-time dissolved oxygen analyzer to detect the generated O_2, and co-incubated MSNPs-SN with Dulbecco's Modified Eagle Medium (DMEM) medium containing 10% Fetal Bovine Serum (FBS). The study sets up AP group, MSNPs-SN group, and MSNPs-SN+NIR group. During the incubation process, the dynamic changes in H_2O_2 concentration in the solution are monitored in real-time using the H_2O_2 detection method and fluorescent probe method [17].

2.3.2. Thermal performance testing

The photothermal performance was evaluated by recording the temperature changes of MSNPs-SN solutions under NIR laser irradiation and over multiple on/off cycles [18].

2.3.3. In vitro cell testing

Cultivate mouse tumor cells A549 in a suitable DMEM medium containing 10% FBS, with an environment set at 37℃ and 5% CO_2 incubator [19]. Inoculate

cells with good growth status into a 96 well plate, and after the cells adhere to the wall, replace them with culture media containing different concentrations of experimental group materials (i.e. intact MSNPs-SN group, blank carrier group without AP and IR825, group without IR825, group without AP) for incubation. Set different concentrations, place the 96 well plate back into the incubator, and incubate for 24 hours and 48 hours, respectively.

2.3.4. In vivo testing of experimental animals

Using the same batch of female experimental mice, A549 lung cancer cells are inoculated under the armpits of the mice. The experiment begins after the tumor grows to a measurable volume. The experiment is divided into 7 groups, namely the control group, MSNPs-SN without IR825 (Group 1), NIR+MSNPs-SN without IR825 (Group 2), MSNPs-SN without AP (Group 3), NIR+MSNPs-SN without AP (Group 4), intact MSNPs-SN (Group 5), and NIR+intact MSNPs-SN (Group 6). All seven groups are intravenously injected with 10mg/kg on the day before the start of the experiment, the 5th day, and the 10th day. Groups 2, 4, and 6 are uniformly irradiated with NIR laser at 800nm and 2.0W/cm^2 for 5 minutes.

3. Results and analysis

3.1. Characterization and performance testing of nanomaterials

To analyze the molecular structure and chemical environment of β-HACD in NDDS, its hydrogen spectrum and Gel Permeation Chromatography (GPC) are analyzed. Three types of tests are shown in Fig. 3.

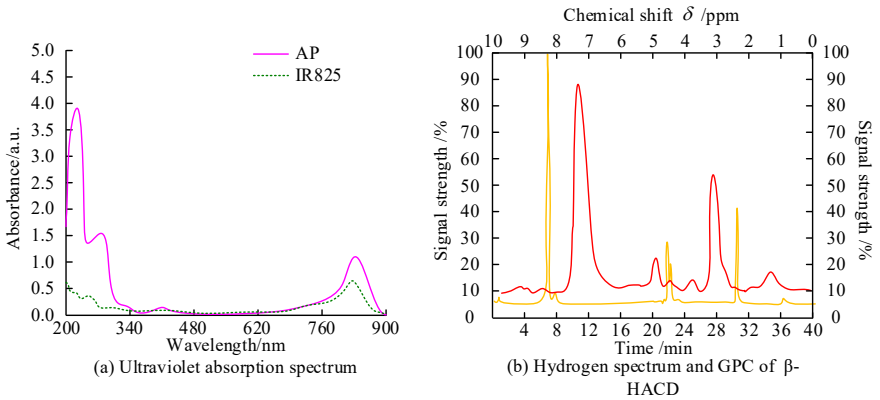

Fig. 3. Performance comparison of AP, IR825, and β-HACD

In Fig. 3 (a), after using the synthesized IR825 standard for full wavelength scanning, it was confirmed that IR825 had a strong absorption peak at 830nm, with

an absorbance of 0.650a.u. This indicates the presence of free AP and IR825 in the supernatant. In Fig. 3 (b), the strong peak on the left side at δ =8.2~8.4ppm and the peak at δ =2.2~2.5 ppm.

To analyze the H_2O_2 production ability of MSNPs-SN, the changes in H_2O_2 concentration after incubation with DMEM containing 10% FBS are shown in Fig. 4.

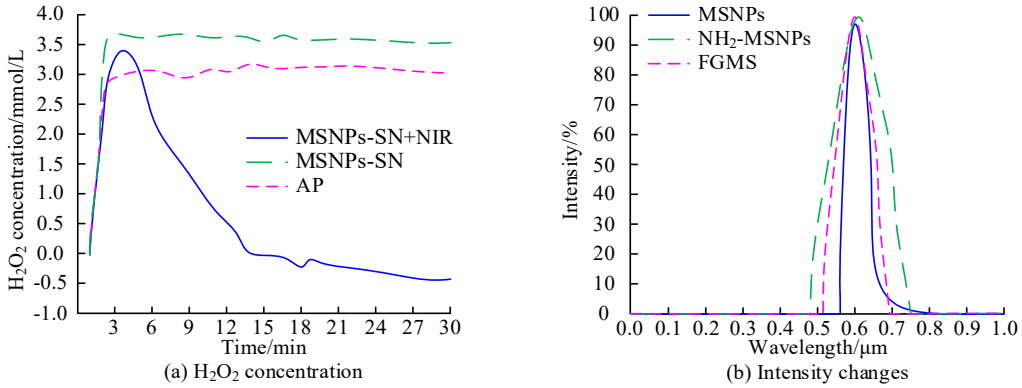

Fig. 4. Change in H_2O_2 concentration

In Fig. 4 (a), the content of MSNPs-SN+NIR, MSNPs SN, and AP increased the fastest in the first 4 minutes. The H_2O_2 concentration of MSNPs-SN increased the most, from 0 to 3.65 mmol/L. Within 4 to 30 minutes, the H_2O_2 concentration of SN remained relatively stable at 3.65 mmol/L. In Fig. 4 (b), the H_2O_2 concentration of MSNPs-SN+NIR rapidly decreased from 4 to 14 minutes until 30 minutes, and the decreasing curve changed, resulting in a negative H_2O_2 concentration. This is because AP undergoes an oxidation reaction with its proteins, leading to an increase in concentration, while NIR can accelerate the consumption of H_2O_2 through the Fenton reaction induced by $Fe(C_5H_5)_2$.

3.2. Application effect testing of MSNPs-SN

To analyze the photothermal efficiency of MSNPs-SN, the temperature changes of different concentrations MSNPs-SN over time are tested, as shown in Fig. 5.

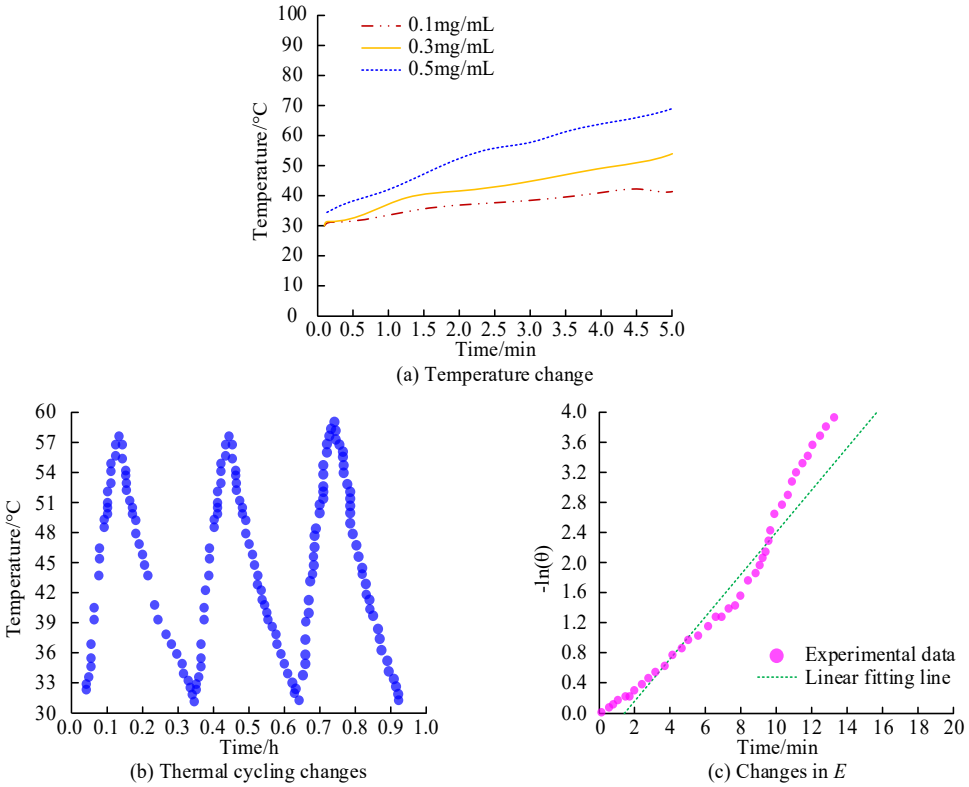

Fig. 5. Photothermal analysis of MSNPs-SN

Fig. 5 (a) shows the temperature variation of different MSNPs-SN concentrations over time. MSNPs-SN exhibited concentration dependent heating behavior, with temperature differences of 11℃, 23℃, and 36℃ for MSNPs-SN at concentrations of 0.1mg/mL, 0.3mg/mL, and 0.5mg/mL after 5 minutes of irradiation at 800nm. Fig. 5 (b) shows the photothermal cycling changes of MSNPs-SN over a period of 1 hour. MSNPs-SN underwent 3 cycles of photoexcitation heating - stopping photoexcitation cooling. In each cycle, the temperature rapidly increased (photothermal conversion stage) and then decreased (heat dissipation stage). MSNPs-SN can effectively limit the degradation of IR825 to enhance photothermal stability. Fig. 5 (c) shows the time - negative logarithmic transmittance - ln(θ) relationship of MSNPs-SN photothermal conversion. Among them, the photothermal conversion efficiency E was 32.4%. Overall, MSNPs-SN material has good photothermal stability and can be used for photothermal enhanced CDT/PDT.

To verify the in vitro toxicity of the material on A549 cells, the cell viability of cells treated with four experimental groups at different concentrations for 24 and 48 hours was studied and analyzed, as shown in Fig. 6.

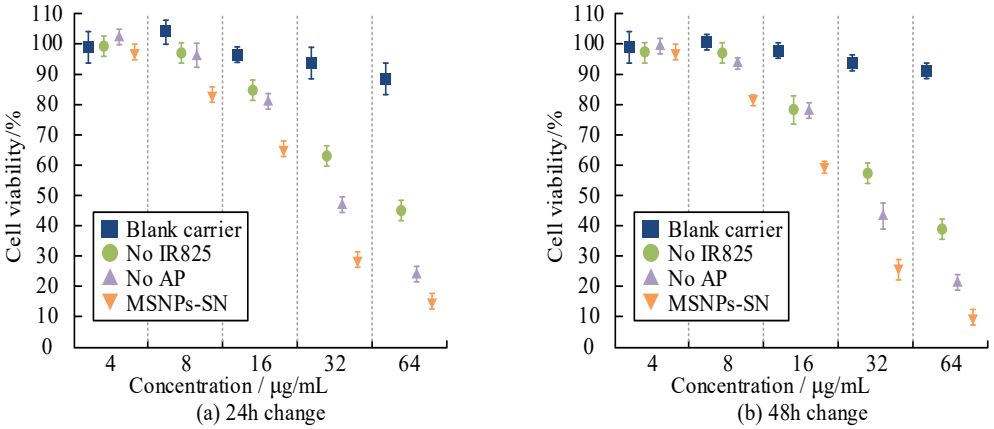

Fig. 6. Changes in tumor cell viability

In Fig. 6 (a), as the concentration of MSNPs-SN increased, the tumor cell viability of the four groups gradually decreased. After 24 hours of treatment, when the concentration of the formulation was 64μg/mL, the tumor cell viability of the blank carrier group was 89.5%, the group without IR825 was 48.6%, the group without AP was 24.1%, and the MSNPs-SN group was 15.8%. In Fig. 6 (b), after 48 hours of treatment, when the concentration of the formulation was 64μg/mL, the tumor cell viability of the blank carrier group was 91.6%, the group without IR825 was 38.4%, the group without AP was 22.5%, and the MSNPs-SN group was 10.2%.

To verify the anticancer effect of the designed MSNPs-SN in vivo, female mice from the same batch are selected for the experiment. The body weight, Relative Tumor Volume (RTV), and weight changes of different groups of experimental mice are shown in Fig. 7.

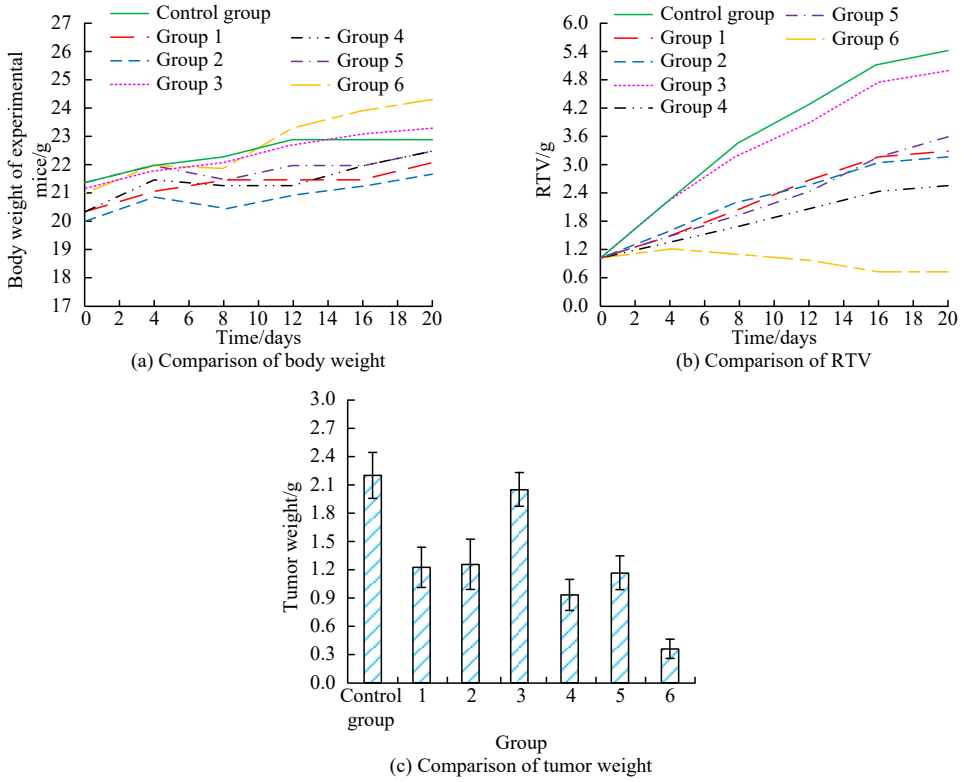

Fig. 7. Body weight, RTV, and weight changes of experimental mice

In Fig. 7 (a), the experimental mice showed a slow increase in body weight from day 0 to day 20 in Group 7, but the difference in changes was not significant. In Fig. 7 (b), the RTV of Group 6 gradually decreased around the 4th day, which was significantly different from the control group (p<0.05). The RTV of Group 5 was statistically significant (p<0.05) compared to the control group. In Fig. 7 (c), compared with the control group, Group 6 showed a significant reduction in tumor weight (p<0.001), while Groups 4 and 5 had significant reductions in tumor weight (p<0.05).

4. Discussion and summary

To enable NDDS to self-replenish reaction substrates, possess multi-source reactive oxygen species generation ability, and achieve efficient tumor targeting, CDT and PTT were combined to design an NDDS. The design idea of this study echoes with a variety of advanced nano drug delivery system strategies in the near future, and has achieved deepening or expansion in the specific direction. For example, similar to literature [5] using natural small molecule self-assembly to improve drug delivery performance, and literature [8] using preparation

engineering to achieve transdermal drug release, this study is also committed to solving the problem of efficient loading and controlled release of drugs (AP/IR825) through precise nanostructure design. More importantly, in terms of NDDs design for specific disease microenvironment, the work of this paper can be compared with the responsive probe designed for H_2O_2 microenvironment in atherosclerotic plaque in literature [6] and the bionic nanoparticles constructed to overcome the blood-brain barrier in literature [9], which all reflect the core logic of customized design based on the characteristics of pathological microenvironment.

Specifically, in the field of combination therapy of CDT and PTT, this study has formed a meaningful contrast and complement with a variety of collaborative strategies reported in the recent literature. For example, literatures [10] and [12] respectively applied the cdt/ptt strategy to the field of antibacterial and anti biofilm, showing the wide applicability of this joint mode, but its mechanism of action mainly relies on the inherent catalytic and photothermal properties of nanomaterials. In contrast, the pH responsive H_2S gas synergistic therapy platform constructed in literature [13] and the fiber-optic in-depth drug delivery combined with heat shock protein inhibition strategy adopted in literature [14] represent more complex and cutting-edge exploration in overcoming the limitations of tumor microenvironment. However, these systems may still depend on the endogenous H_2O_2 level of tumor or require complex external equipment and multi-step synthesis process.

In contrast, in the proposed NDDS, MSNPs-SN rapidly increased the H_2O_2 concentration to 3.65mmol/L within 4 minutes and tended to stabilize, creating a CDT reaction environment. The NDDS constructs a multi-modal, multi-reactive oxygen species synergistic therapy system with photothermal enhancement, rather than a simple parallel functional system. Under NIR light irradiation, the concentration of MSNPs-SN+NIR group sharply decreased within 4-14 minutes and decreased to negative values after 30 minutes, indicating that AP could sustainably supply H_2O_2, while light significantly accelerated its consumption through Fenton reaction. The photothermal effect induced by NIR irradiation not only directly ablates tumors, but also significantly accelerates the Fenton reaction kinetics due to local heating. This study has successfully provided effective strategies for overcoming the limitations of tumor microenvironment and achieving multimodal collaborative therapy. However, there is still room for optimization in drug encapsulation efficiency and release control, and the long-term safety in vivo has not been fully evaluated. Future work will focus on improving load efficiency, conducting in vivo efficacy and toxicity evaluations of the system, and exploring the potential application of this system in combination immunotherapy.

Fundings

The research is supported by: General Project of National Natural Science Foundation of China (82072229); National Natural Science Foundation of China Youth Science Foundation (82104375); 2025 Science and Technology Plan Project of Shaanxi Provincial Department of Science and Technology (2025JC-YBMS962); Shaanxi Provincial Department of Education 2023 General Special Scientific Research Plan Project (23JK0585).

REFERENCES

[1] *J. Liu, J. Liu, W. Mu, Q. Ma, X. Zhai, B. Jin, Y. Liu, N. Zhang,* Delivery strategy to enhance the therapeutic efficacy of liver fibrosis via nanoparticle drug delivery systems, ACS Nano, Vol. **18**, Iss. 32, 2024, 20861-20885, DOI: 10.1021/acsnano.4c02380.

[2] *X. Liu, Y. Cao, S Wang, J. Liu, H. Hao,* Extracellular vesicles: powerful candidates in nano-drug delivery systems, Drug Delivery and Translational Research, Vol. **14**, Iss. 2, 2024, 295-311, DOI: 10.1007/s13346-023-01411-x.

[3] *P. Theivendren, S. Kunjiappan, P. Pavadai, K. Ravi, A. Murugavel, A. Dayalan, A. Santhana Krishna Kumar,* Revolutionizing cancer immunotherapy: emerging nanotechnology-driven drug delivery systems for enhanced therapeutic efficacy, ACS Measurement Science Au, Vol. **5**, Iss. 1, 2024, 31-55, DOI: 10.1021/acsmeasuresciau.4c00062.

[4] *X. Zhai, S. Peng, C. Zhai, S. Wang, M. Xie, S. Guo, J. Bai,* Design of nanodrug delivery systems for tumor bone metastasis, Current Pharmaceutical Design, Vol. **30**, Iss. 15, 2024, 1136-1148. DOI: 10.2174/0113816128296883240320040636.

[5] *Q. Li, Y. Lianghao, G. Shijie, W. Zhiyi, T. Yuanting, C. Cong, C.Q. Zhao, F. Xianjun,* Self-assembled nanodrug delivery systems for anti-cancer drugs from traditional Chinese medicine. Biomaterials Science, 2024, **12**(7): 1662-1692. DOI:10.1039/D3BM01451G.

[6] *M. Shen, H. Jiang, S. Li, L. Liu, Q. Yang, H. Yang, Y. Zhao, H. Meng, J. Wang, Y. Li,* Dual-modality probe nanodrug delivery systems with ROS-sensitivity for atherosclerosis diagnosis and therapy, Journal of Materials Chemistry B, Vol. **12, Iss.** 5, 2024, 1344-1354, DOI: 10.1039/D3TB00407D.

[7] *D. Birla, N. Khandale, B. Bashir, M. ShahbazAlam, S. Vishwas, G. Gupta, S.K. Singh, et al.* Application of quality by design in optimization of nanoformulations: Principle, perspectives and practices, Drug Delivery and Translational Research, Vol. **15**, Iss. 3, 2025, 798-830, DOI: 10.1007/s13346-024-01681-z.

[8] *R. Mirza, K.U. Shah, A.U. Khan, M. Fawad, A.U. Rehman, N. Ahmed,A. Nawaz, S.U. Shah, A.F. Alasmari, M. Alharbi, F. Alasmari, Z. Hafeez, S.U. Haq,* Statistical design and optimization of nano-transfersomes based chitosan gel for transdermal delivery of cefepime. Drug Development and Industrial Pharmacy, Vol. **50**, Iss. 6, 2024, 511-523, DOI: 10.1080/03639045.2024.2353098.

[9] *C. Yan, J. Gu, S. Yin, H. Wu, X. Lei, F. Geng, N. Zhang, X. Wu,* Design and preparation of naringenin loaded functional biomimetic nano-drug delivery system for Alzheimer's disease, Journal of Drug Targeting, Vol. **32**, Iss. 1, 2024, 80-92, DOI: 10.1080/1061186X.2023.2290453.

[10] *J. Wu, S. Xiang, M. Zhang, N. Zhou, M. Wang, L. Li, J. Shen,* Self-assembled nanoflowers realizes synergistic sterilization with photothermal and chemical kinetics therapy, Langmuir, Vol. **40**, Iss. 5, 2024, 2591-2600, DOI: 10.1021/acs.langmuir.3c02838.

[11] *X.X. Wu, D.H. Zhang, Y.N. Ding, F. Cao, Y. Li, J.L. Yao, X.Y. Miao, L.L. He, J. Luo, J.W. Li, J. Lin, A.G. Wu, J.P. Zheng,* Self-assembled co-delivery system of gold nanoparticles and paclitaxel based on in-situ dynamic covalent chemistry for synergistic chemo-photothermal therapy, Rare Metals, Vol. **44**, Iss. 1, 2025, 417-429, DOI: 10.1007/s12598-024-03047-3.

[12] *G. Qian, Y. Mao, H. Zhao, L. Zhang, L. Xiong, Z. Long,* pH-Responsive nanoplatform synergistic gas/photothermal therapy to eliminate biofilms in poly (L-lactic acid) scaffolds, Journal of Materials Chemistry B, Vol. **12**, Iss. 5, 2024, 1379-1392, DOI: 10.1039/D3TB02600K.

[13] *G. Ma, X. Zhang, K. Zhao, S. Zhang, K. Ren, M. Mu, C.Wang, X. Wang, H. Liu, J. Dong, X. Sun,* Polydopamine nanostructure-enhanced water interaction with pH-responsive manganese sulfide nanoclusters for tumor magnetic resonance contrast enhancement and synergistic ferroptosis-photothermal therapy, ACS Nano, Vol. **18**, Iss. 4, 2024, 3369-3381, DOI: 10.1021/acsnano.3c10249.

[14] *Z. Zhang, X. Yue, N. Lan, Y. Zhang, Z. Li, F. Jin, Y. Wang, B. Guan, Y. Ran, K. Liu,* Effective antitumor synergistic treatment with fiber-photothermal therapy and heat shock protein inhibitors, ACS Applied Materials & Interfaces, Vol. **17**, Iss. 3, 2024, 4368-4379, DOI: 10.1021/acsami.4c11734.

[15] *H. Mazumdar, K.R. Khondakar, S. Das, A. Halder, A. Kaushik,* Artificial intelligence for personalized nanomedicine; from material selection to patient outcomes, Expert Opinion on Drug Delivery, Vol. **22**, Iss. 1, 2025, 85-108, DOI: 10.1080/17425247.2024.2440618.

[16] *V.S. Gharge, M.B. Shinde, S.L. Jadhao, S.N.P. Sadamat, N.S. Biradar*, Multivariate analysis and computational predictability of modified release formulation of chirally pure metoprolol succinate, Archives of Advanced Engineering Science, Vol. **2**, Iss. 3, 2024, 160-169, DOI: 10.47852/bonviewAAES3202137.

[17] *X. Chen, F. Zhang, C. Lu, R. Wu, B. Yang, T. Liao*, Lactate-fueled theranostic nanoplatforms for enhanced MRI-guided ferroptosis synergistic with immunotherapy of hepatocellular carcinoma, ACS Applied Materials & Interfaces, Vol. **17**, Iss. 6, 2025, 9155-9172, DOI: 10.1021/acsami.4c21890.

[18] *S. Rajendran, S.N. Ravi, V.M. Nair, R.P. Sree, A.S.B. Packirisamy, J. Palanivelu*, Recent development and future aspects: nano-based drug delivery system in cancer therapy, Topics in Catalysis, Vol. **67**, Iss. 1, 2024, 203-217, DOI: 10.1007/s11244-023-01893-6.

[19] *E. Dong, Q. Huo, J. Zhang, H. Han, T. Cai, D. Liu*, Advancements in nanoscale delivery systems: optimizing intermolecular interactions for superior drug encapsulation and precision release, Drug Delivery and Translational Research, Vol. **15**, Iss. 1, 2025, 7-25, DOI: 10.1007/s13346-024-01579-w.